Erosional Cyclic Steps Governed by Plunge Pool Erosion
A Parametric Study Based on Field, Laboratory, and Model Data

Zeng, Xin; Blom, Astrid; Czapiga, Matthew J.; An, Chenge; Parker, Gary; Fu, Xudong

DOI
10.1029/2020JF006034

Publication date
2021

Document Version
Final published version

Published in
Journal of Geophysical Research: Earth Surface

Citation (APA)
Zeng, X., Blom, A., Czapiga, M. J., An, C., Parker, G., & Fu, X. (2021). Erosional Cyclic Steps Governed by Plunge Pool Erosion: A Parametric Study Based on Field, Laboratory, and Model Data. *Journal of Geophysical Research: Earth Surface*, *126*(11), Article e2020JF006034. https://doi.org/10.1029/2020JF006034

JGR Earth Surface

RESEARCH ARTICLE
10.1029/2020JF006034

Key Points:

- Length and height of cyclic steps increase with flow rate in measured data and model predictions
- Smaller channel slope and larger bed erodibility result in a larger step aspect ratio in measured data and model predictions
- Adding plunge pool erosion improves model predictions for step length, height, and aspect ratio relative to the average channel slope

Supporting Information:

Supporting Information may be found in the online version of this article.

Correspondence to:

X. Fu and C. An,
xdfu@tsinghua.edu.cn;
anchenge08@163.com

Citation:

Zeng, X., Blom, A., Czapiga, M. J., An, C., Parker, G., & Fu, X. (2021). Erosional cyclic steps governed by plunge pool erosion: A parametric study based on field, laboratory, and model data. *Journal of Geophysical Research: Earth Surface*, *126*, e2020JF006034. https://doi.org/10.1029/2020JF006034

Received 16 DEC 2020
Accepted 28 OCT 2021

Erosional Cyclic Steps Governed by Plunge Pool Erosion: A Parametric Study Based on Field, Laboratory, and Model Data

Xin Zeng[1,2], Astrid Blom[2], Matthew J. Czapiga[2], Chenge An[1], Gary Parker[3], and Xudong Fu[1]

[1]Department of Hydraulic Engineering, State Key Laboratory of Hydroscience and Engineering, Tsinghua University, Beijing, China, [2]Department of Hydraulic Engineering, Faculty of Civil Engineering and Geosciences, Delft University of Technology, Delft, The Netherlands, [3]Department of Civil and Environmental Engineering and Department of Geology, University of Illinois, Urbana-Champaign, IL, USA

Abstract For upland ephemeral gullies, gully erosion is strongly related to the formation and migration of cyclic steps. It is necessary to provide insight into the process of cyclic step development to accurately predict the pace of landscape evolution and soil loss. Information on the geometry of cyclic steps in subaerial environments is limited, and, to our knowledge, no model of cyclic step development considers plunge pool erosion. In this study, we analyze the geometric features and controlling factors of erosional cyclic steps through meta-analysis of measured data including new measurements in the Loess Plateau, China. We focus on cyclic step dynamics of fluvial beds controlled by bed shear stress and local plunge pool erosion. We develop a new theory to incorporate plunge pool erosion through adapting existing cyclic step and plunge pool models. Our method agrees with measured data, showing that a larger flow rate leads to larger step length L_d and height H_d and increasing erodibility increases step aspect ratio L_d/H_d. The method is also able to predict how the step length, height, and aspect ratio change with the average channel slope. Our results indicate that plunge pool erosion is an important mechanism of cyclic step evolution. However, plunge pool development alone is not sufficient to explain the wide range of L_d/H_d in the measured data. The posed theory relates to equilibrium conditions and thus cannot consider temporal adjustments in step geometry.

Plain Language Summary The beds of upland ephemeral gullies often have long profiles with a discontinuous series of upstream-migrating steps. Channels with these steps show characteristics of water flow and sediment transport that differ from channels where steps are absent. This difference in turn affects the rates of landscape evolution and soil erosion. In the Loess Plateau, China, periodic steps are accompanied by plunge pool erosion below a free overfall. No models to date tie both step and plunge pool formation. In this study, we present geometric data of steps measured in a small watershed of the Loess Plateau. We develop a theory that models periodic steps with plunge pool erosion. We identify the factors that control step geometry through meta-analysis of measured data and numerical modeling. The results show that discharge, bed erodibility, and slope are coupled with each other in the establishment of step-pool geometry. Furthermore, we find that plunge pool erosion is a key mechanism that controls the trend between step height and slope. However, the new model fails to completely describe the wide range of values of step length divided by step height, probably because it does not consider the change in step geometry over time.

1. Introduction

Cyclic steps are step-like bedforms that have been observed on alluvial fans, cohesive beds, exposed bedrock, seafloor, and ice (Kostic et al., 2010; Slootman & Cartigny, 2020). Each step is characterized by a gently sloping stoss section, followed immediately by a steep lee section downstream (Fagherazzi & Sun, 2003; Izumi et al., 2017; Winterwerp et al., 1992). The flow is subdivided into alternating zones of subcritical flow along the flatter slope and supercritical flow along the steeper slope (Kostic & Parker, 2006; Parker, 1996; Yokokawa et al., 2009). Cyclic steps are long-wave bedforms bounded by hydraulic jumps, which migrate

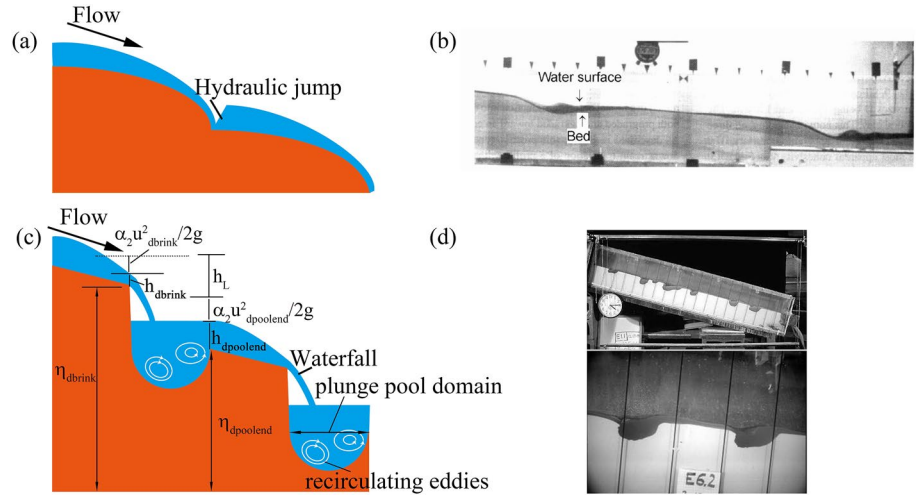

Figure 1. (a) Type I cyclic steps (no pool) are separated by a hydraulic jump occurring immediately downstream of the step's steep lee slope. (b) Two Type I steps are shown with associated hydraulic jumps (Taki & Parker, 2005). (c) Type II cyclic steps (with pool) have a near-vertical lee slope where flow detaches from the bed and impinges the downstream bed, developing a plunge pool, which then dissipates energy. (d) Two Type II steps, with downstream plunge pools are shown in the experiments conducted by Brooks (2001).

upstream due to erosion at the toe of each step (Fildani et al., 2006; Slootman & Cartigny, 2020; Sun & Parker, 2005).

Cyclic steps are comparable to step pool systems, which have been more broadly researched in the past. Both morphologies relate to spatial transitions in flow regime between subcritical and supercritical flow via hydraulic jumps (Church & Zimmermann, 2007; Slootman & Cartigny, 2020). Step pool systems have a wider grainsize distribution than cyclic steps (Brooks, 2001). In step pool systems, steps are constructed with cobbles and boulders and finer sediments deposit in pools. Their geometry depends primarily on the average channel slope and sediment supply (Chin & Wohl, 2005; Recking et al., 2012; Waters & Curran, 2012; Wohl & Grodek, 1994). Cyclic steps, however, can form autogenically on homogeneous bed surfaces of uniform bed material (Balmforth & Vakil, 2012; Parker & Izumi, 2000). Many ideas of step pool formation rely on grain sorting, which are therefore not directly applicable to cyclic steps.

Regardless, both morphologies rely on hydraulic instabilities that self-perpetuate their form. Of the proposed theories for step pool development, we focus on those that highlight hydraulic instabilities. The widely used "Antidune Model" suggests that step pools form via antidunes when a cluster of large particles stall on the upstream face of each antidune and accumulate more deposition around it (Curran, 2007; Grant, 1994; Recking et al., 2009; Whittaker & Jaeggi, 1982). Alternatively, step pools have been observed to form more randomly when important keystones deposit and promote further deposition of other particles (Curran & Wilcock, 2005; Golly et al., 2019; Judd & Peterson, 1969; Zimmermann & Church, 2001). In both cases, the deposition of large particles invokes a change in flow regime, which then promotes further stabilization of step pools. In contrast to step pools, cyclic steps can form without large particles. Parker and Izumi (2000) applied the linear stability analysis to explain the formation of erosional cyclic steps. They found that cyclic steps can form spontaneously under supercritical flow due to instabilities of flow hydraulics and bed erosion. Cyclic steps can still exist for subcritical flow but need to be triggered by an initial finite-amplitude perturbation (Parker & Izumi, 2000). Furthermore, the analysis of nonlinear dynamics of cyclic steps shows that roll waves, a second instability of supercritical flow, render steadily migrating steps less regular and time dependent (Balmforth & Vakil, 2012).

We further divide cyclic step geometry into two categories relative to the absence (Type I) and presence (Type II) of a plunge pool immediately downstream of the step (Figure 1). Formation and migration of Type I cyclic steps (no pool) are controlled by fluvial erosion caused by excess bed shear stress. These steps are typically found on erodible beds of silt or sand (Taki & Parker, 2005; Winterwerp et al., 1992). Flow

accelerates from subcritical flow to supercritical flow until a hydraulic jump occurs between two successive steps (Figure 1a).

Type 1 step geometry depends on sediment grainsize and the sediment transport rate. The step lee face (or supercritical flow region) flattens with increasing grainsize (from silt to sand) (Taki & Parker, 2005). Step length increases as sediment transport rate increases, and the migration rate of steps decreases as inflow sand concentration increases (Winterwerp et al., 1992).

Theoretical models of Type I steps use the St. Venant equations under the assumption of a hydraulic jump on gentle slopes (Fagherazzi & Sun, 2003; Izumi et al., 2017; Parker & Izumi, 2000; Sun & Parker, 2005). One of the most widely used models for Type I steps is the Parker and Izumi (2000) model, which eliminates deposition by assuming eroded bed sediment no longer interacts with the bed, that is, washload. Under such conditions, cyclic step geometry is controlled by two Froude numbers relative to: (a) the normal flow condition in the absence of steps and (b) the threshold velocity for bed erosion (Parker & Izumi, 2000), illustrating the importance of channel slope and bed erodibility on step geometry.

Type II cyclic steps have plunge pools (Figure 1b) and their development depends on both fluvial erosion and plunge pool erosion via free-falling water over the step crest (Brooks, 2001; Grimaud et al., 2016; Scheingross et al., 2019). Type II steps have been studied experimentally in soils with varying cohesion (Ashida & Sawai, 1977; Brooks, 2001; Koyama & Ikeda, 1998) and in bedrock of varying strength (Grimaud et al., 2016). Yet, most focus has been placed on controls of cyclic step morphology in bedrock. Similar to Type I steps, the channel slope strongly controls the step length, height, and aspect ratio of Type II steps in bedrock (Wohl & Grodek, 1994). Temporal alluvial cover and sediment supply also play a role in step formation of bedrock cyclic steps (Grimaud et al., 2016; Scheingross et al., 2019), where plunge pool depth is also strongly influenced by bedrock lithology (Grimaud et al., 2016).

Conceptual models quantify the overall headcut retreat by considering vertical incision or knickpoint undercutting in bedrock (Lamb et al., 2007; Scheingross & Lamb, 2017) or plunge pool erosion of soil beds (Alonso et al., 2002; Flores-Cervantes et al., 2006; Stein et al., 1993). Among them, the Flores-Cervantes et al. (2006) model assumes a fixed pool shape during headcut migration, but accounts for flow discharge, headcut height, upstream slope, bed roughness, and various soil properties.

In the Loess Plateau, cyclic steps form in loess, a special weakly cohesive deposit with particle composition ranging from sand to clay (Luo, 2015; Wang et al., 2000). Under dry conditions, loess has a large shear strength and can stand vertically, but when it becomes wet, it is easily eroded by flow (Luo, 2015). Given this particularity of loess, the cyclic steps in the Loess Plateau present headcuts and underlying plunge pools (Figure S8 in the Supporting Information S1). Existing data sets of cyclic steps come from channels with cohesive sediments or bedrock, so our data set expands the existing domain of observed measurements in terms of bed erodibility (much larger erodibility under wet condition) to include steps in weakly cohesive loess. Loess cyclic steps may exhibit different morphological features than those previously observed in cohesive or bedrock materials. Neither the Flores-Cervantes et al. (2006) model nor the Parker and Izumi (2000) model can be applied alone to the Type II cyclic steps in loess due to the coupled nature of fluvial erosion and plunge pool erosion.

Cyclic steps and headcut erosion control the production of sediment in upland ephemeral gullies. Plunge pool erosion, as a driver of headcut retreat, then significantly influences the morphodynamic characteristics of cyclic steps on bedrock, strongly cohesive beds, or weakly cohesive beds, like loess gullies. Therefore, understanding the processes of cyclic step retreat are critical to accurately predict the pace of landscape evolution, soil loss, and sediment sourcing into lowland streams. The objective of this paper is to characterize the geometric features and controlling physics of subaerial, erosional cyclic steps accompanied by plunge pool erosion (Type II), and to develop a theory that can predict erosional cyclic steps with plunge pools. We collect and analyze a variety of field and laboratory data sets on erosional steps ranging from weakly cohesive sediments to bedrock. As a first-order approximation, we adapt and combine the Parker and Izumi (2000) model for equilibrium cyclic steps and the Flores-Cervantes et al. (2006) model for plunge pool erosion. We test the performance of the adapted model by comparing the simulations with the observations in measured data.

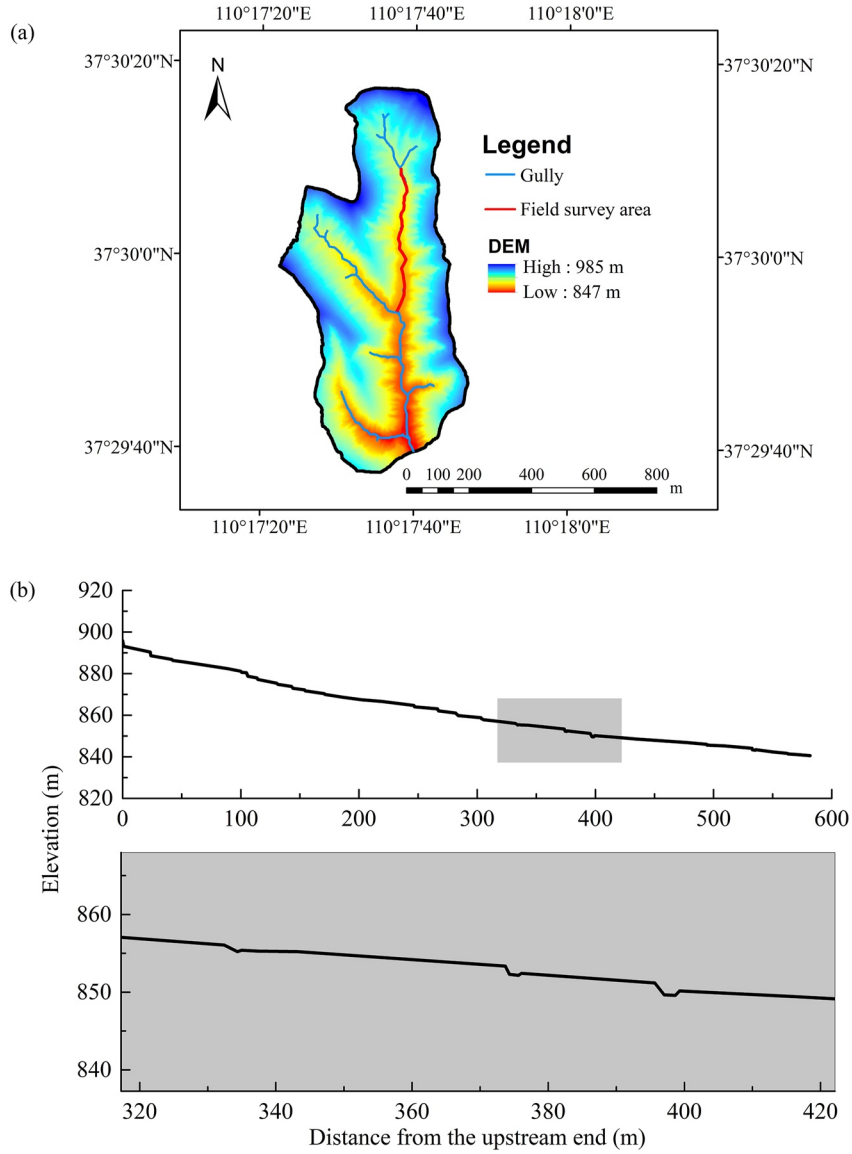

Figure 2. (a) Location of our study sites in the Qiaogou watershed and three main tributaries within this watershed. (b) Measured bed level of the Qiaogou mainstem in our field survey area as shown in Figure 2a.

2. Study Site and Data

2.1. Study Area and Data Collection in the Loess Plateau

The study sites lie in Wuding River Basin of the Loess Plateau, China. The climate is a typical monsoon climate, with the majority of the precipitation concentrated between June and September. We measure cyclic steps in the Qiaogou watershed, yet steps are ubiquitous in steep gullies throughout the Loess Plateau. The Qiaogou watershed (latitude 37°29′40″N-37°30′20″N, longitude 110°17′20″E–110°17′30″E) covers a drainage area of 0.45 km^2 (Wang et al., 2018), and the main stem length is 1.4 km with two main tributaries. Steps are measured in a sub-channel with a length of about 600 m in the mainstem as shown in Figure 2a. The soils have a fine-silty texture that is susceptible to water erosion (Zeng et al., 2015).

We performed a field survey in the mainstem as shown in Figure 2a. Measured cyclic steps range in height from less than 1 m to nearly 8 m (Figure S8 in the Supporting Information S1 shows the 8 m step). Step spacing tends to decrease in the upstream direction. Headcut slope shows a wide range, with values up to 74 degrees (Figure S9 of the Supporting Information S1). The angle of repose of friable loess is approximately

Table 1
Description of the Data Sets on Erosional Steps Used in This Study

Reference	Channel width	Slope	Bed material	Discharge
Flume				
Koyama & Ikeda (1998)	2.5–5 cm	5%–143%	Weakly cohesive material	66 cm^3/s
Brooks (2001)	4.9 cm	14.8%–36.2%	Strongly cohesive material	125–225 cm^3/s
Field				
Wohl & Grodek (1994)	10–240 cm	3.5%–100%	Bedrock	Peak discharge varies between 0.83 and 1.07 m^3/s.
Our data in Qiaogou	72–398 cm	5%–143%	Weakly cohesive loess	Peak discharge = 2.30 m^3/s; Average flood discharge = 0.25 m^3/s.

38 degrees, implying that steep headcuts exceeding the angle of repose may be prone to failure if vertical undercutting continues (Lohnes & Handy, 1968). In addition to these steep scarps, during floods, a jet flow impinges the bed downstream of the step and plunge pool erosion occurs when the shear stress of the jet flowing into the plunge pool exceeds the threshold shear stress of the weakly cohesive silty loess. Once eroded, we consider silt to be a washload sediment that is convected out of the study domain without interacting with the bed surface. Deposition only occurs in plunge pools where extensive energy dissipation occurs.

2.2. Other Data Sets From Field and Lab Experiments

Wohl and Grodek (1994) investigated multiple steps in ephemeral reaches of boulder and bedrock streams. Cyclic steps in bedrock can be regarded as erosional, and thus comparable with our field data sets of weakly cohesive erosional steps. Laboratory experiments of erosional cyclic steps dominated by both fluvial erosion and plunge pool erosion have also been included in the analysis (Brooks, 2001; Koyama & Ikeda, 1998). A brief description of the data sets used in this study is presented in Table 1 and step length and step height are shown in Table S1–Table S4 in the Supporting Information S1.

Only data sets that include plunge pool erosion (Type II cyclic steps) are used in this study. All experiments by Brooks (2001) developed Type II cyclic steps (with pool). Koyama and Ikeda (1998) note that small waterfalls develop when average bed slope exceeded 6 degrees (10.5%). We use this as a criterion for plunge pool development and remove all lower-slope data from the Koyama and Ikeda (1998) data. The Wohl and Grodek (1994) data set includes both bedrock steps and alluvial steps. Here, we only use their bedrock steps for analysis. Ashida and Sawai (1977) also conducted experiments on erosional steps, but these data are omitted as plunge pool erosion is limited in their experiments and only occurred via potholes at slopes exceeding 50%.

Our compendium of data covers a wide range of average channel slopes from 3.5% to 143%. Bed material in these data sets varies from weakly cohesive bed to bedrock. A constant flow rate was imposed at the upstream end of the flume in all experiments, and flow rate ranged from 66 cm^3/s to 225 cm^3/s.

Cyclic step development from incipient formation to equilibrium shape varies throughout the collected data set. Koyama and Ikeda (1998) ran experiments until a steady erosion rate is met, which implies a quasi-equilibrium state. However, quasi-equilibrium is not met in other data sets. Brooks (2001) showed that cyclic steps tend to coalesce toward the end of experiments, suggesting cyclic steps may not have met equilibrium. Wohl and Grodek (1994) reported that cyclic step height and length systematically vary from downstream to upstream, suggesting all steps in their data are still evolving. Similarly, cyclic steps in the Qioagou region have not reached equilibrium. Step dimensions were measured in September 2017 and June 2018. After one year, we found the channel lengthened as the upstream steps migrated further upslope. Meanwhile new steps developed downstream, and step length and height of all steps adjusted during this period.

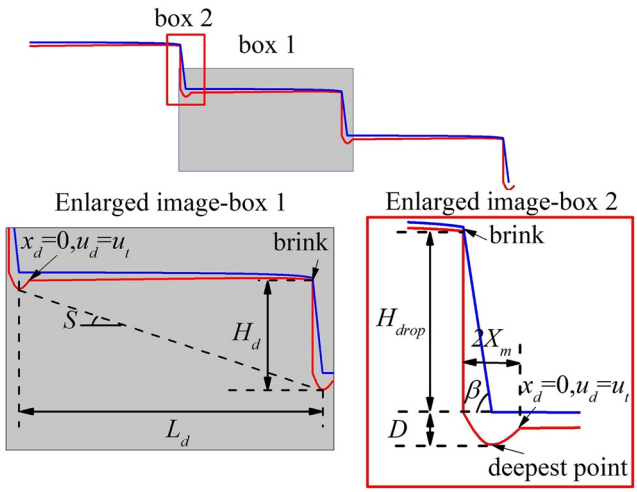

Figure 3. Definitions of cyclic step geometry shown with bed level and water surface level predicted by the plunge pool model. Step geometry includes both the step and plunge pool. Step length L_d is measured between midpoints of adjacent plunge pools and step height H_d includes the step lee face H_{drop} and maximum plunge pool depth D. S is average channel slope when equilibrium solutions of cyclic steps migrating upstream with constant wave velocity are sought. At the downstream lip of the last plunge pool ($x_d = 0$), the dimensional flow velocity u_d equals to the threshold velocity for bed erosion u_t.

3. Model of Erosional Cyclic Steps With Consideration of Plunge Pools

One of the most widely used models to simulate the geometry of purely erosional cyclic steps was developed by Parker and Izumi (2000). The model is simple to apply and also captures the most essential features of cyclic steps in cohesive beds. In this paper, we apply the Parker and Izumi (2000) model as a starting point. In the analysis of the Parker and Izumi (2000) model, dimensionless variables are introduced and the governing equations based on the St. Venant shallow water equations and the Exner equation are transformed into a nonlinear ordinary differential equation of dimensionless flow velocity. With two dimensionless boundary conditions on flow velocities, the Parker and Izumi (2000) model can be solved. The total dimensionless bed degradation rate in the presence of steps differs from that in their absence by a dimensionless additional rate of degradation w_a. w_a is an important parameter that needs to be specified in the Parker and Izumi (2000) model and it should be between an upper bound w_{au} and a lower bound w_{al} in order to allow the existence of the solution of the model. The Parker and Izumi (2000) model is presented in the Supporting Information S1.

Waterfalls are ubiquitous features in erosional cyclic steps, and their upstream migration is likely to be linked with the plunge pool erosion at the base of the headcut. The Parker and Izumi (2000) model does not consider this mechanism. However, Flores-Cervantes et al. (2006) developed a conceptual model for plunge pool development subject to a uniform upstream flow in free fall over a nearly vertical face, that is, a waterfall. With some minor modifications, we are able to graft this model onto the erosional cyclic step model proposed by Parker and Izumi (2000). By combining the models, we are able predict cyclic step geometry including the presence of plunge pools (Type II cyclic steps).

We subdivide each step into two domains: the portion upstream of the brink (from $x_d = 0$ to the brink, with $x_d = 0$ denoting the downstream lip of the plunge pool; Figure 3), and the plunge pool region from the brink to the downstream lip of the plunge pool, which includes the step lee face and plunge pool (Figure 3). Since we assume deposition only occurs in the plunge pools, the upstream region is purely erosional and modeled with the Parker and Izumi (2000) model, and the Flores-Cervantes et al. (2006) model is then applied to the pool region.

Connecting these models requires some modifications to the original Parker and Izumi (2000) model. The base model predicts step geometry between hydraulic jumps, which also includes the step lee face. Therefore, we modify the downstream boundary condition for velocity from the conjugate value of the velocity downstream of a hydraulic jump u_t to the velocity at the brink point u_{dbrink}. As we seek to understand the influence of bed erodibility on cyclic step geometry, we consider parameters that affect the erosion rate in erosional cyclic steps. Erosion rate E (Parker & Izumi, 2000) is defined as:

$$E = \alpha\left(\frac{u_d^2}{u_t^2} - 1\right)^n \tag{1}$$

where α is a constant coefficient; u_d is depth-averaged velocity; u_t is the threshold velocity for bed erosion; and n is the bed erosion rate exponent, ranging from 1 to 4 based on the literature (e.g., Teisson et al., 1993; Umita et al., 1988). We consider threshold velocity u_t and exponent n to be dependent on the bed composition and therefore representative of bed erodibility.

The Flores-Cervantes et al. (2006) model assumes uniform flow over a flat slope upstream of a brink point, which then flows over the brink point into a downstream plunge pool (Figure 3). Flow plunges into the pool below, dissipating energy through turbulent mixing, which describes the turbulent transfer via turbulent fluctuations of thermal-hydraulic parameters (Cheng, 2019). It is assumed that the deepest point of the

pool is at the center of the pool domain, so that the pool geometry can be described by a shape factor that relates pool depth to the half-length of the pool. Pool size is a function of discharge, height of the headcut, bed slope and roughness upstream of the brink point, and soil properties. This model assumes that plunge pool shape remains constant during the migration of the headcut. And the migration rate of the headcut is proportional to the undercutting rate of the pool.

The two models are dependent on one another as the step shape predicted by the Parker and Izumi (2000) model affects the plunge pool shape predicted by the Flores-Cervantes et al. (2006) model and the plunge pool shape affects the step migration rate, which then affects step dimensions. The models are linked by adopting a boundary condition at the brink point for equal migration rate. The migration rate of the step is equal to the retreat rate of the headcut, which is proportional to the undercutting rate of the plunge pool (Flores-Cervantes et al., 2006). The predicted migration rate is applied to the Parker and Izumi (2000) model, which solves the bed profile of the upstream domain (i.e., upstream of the brink). As mentioned in Flores-Cervantes et al. (2006), the pool shape remains constant as the headcut migrates. Altogether, we obtain a series of steady and equilibrium steps with plunge pools at a given imposed average channel slope. When the flow regime upstream of the brink point is subcritical, the velocity at the brink u_{dbrink} can be calculated with the following equation (Flores-Cervantes et al., 2006):

$$u_{\mathrm{dbrink}} = \frac{\sqrt[3]{q_w g}}{0.715} \tag{2}$$

with q_w being the flow discharge per unit width and g is gravitational acceleration. Here, the upstream region is treated as the accelerated zone where flow accelerates toward the free overfall.

The Flores-Cervantes et al. (2006) model is used to calculate the geometry of the plunge pool. The shape factor S_f used to describe the shape of the pool is:

$$S_f = \frac{D}{X_m} \tag{3}$$

where D is the maximum depth of the pool and X_m is the half length of the pool (Figure 3). The shape factor is assumed to be constant as the headcut retreats. The deepening rate of the plunge pool and migration rate of the headcut can be linked to this shape factor:

$$c_{sd} = \frac{1}{S_f}\frac{dD}{dt} \tag{4}$$

Here, c_{sd} is the retreat rate of the headcut, which is equal to the migration rate of the domain upstream of the brink. The deepening rate dD/dt depends on flow velocity at the bottom of the pool u_{dbottom}. The deepening rate can be calculated by

$$\frac{dD}{dt} = \begin{cases} \alpha_1 \left(\rho C_{\mathrm{fpool}} u_{\mathrm{tpool}}^2\right)^n \left(\dfrac{u_{\mathrm{dbottom}}^2}{u_{\mathrm{tpool}}^2} - 1\right)^n & u_{\mathrm{dbottom}} > u_{\mathrm{tpool}} \\ 0 & u_{\mathrm{dbottom}} \le u_{\mathrm{tpool}} \end{cases} \tag{5}$$

where α_1 is a constant coefficient; ρ is water density; C_{fpool} is the bed resistance coefficient in the pool region; and u_{tpool} is the threshold velocity for bed erosion in the pool region. Equation 5 is equivalent to Equation 2 in Flores-Cervantes et al. (2006). The bed resistance coefficient C_{fpool} in the pool region is different from the value C_f upstream of the brink (a user specified constant), and is given as

$$C_{\mathrm{fpool}} = 0.025\left(\frac{\upsilon}{q_{\mathrm{w}}}\right)^{0.2} \tag{6}$$

where ν is the kinematic viscosity of water (Flores-Cervantes et al., 2006). The threshold shear stress for bed erosion τ_{cr} is the same in the pool domain and upstream of the brink, which leads to

$$\tau_{cr} = \rho C_{\text{fpool}} u_{\text{tpool}}^2 = \rho C_f u_t^2 \tag{7}$$

The velocity at the bottom of the pool u_{dbottom} depends on whether the flow condition in the pool represents a "nondiffusion state" or a "diffusion state". This condition is determined relative to two representative lengths: the span where velocity is equal to the velocity at the pool surface J_p (i.e., the threshold distance so that no diffusion of the centerline velocity occurs); and the length along the jet centerline from the impinging point at the pool surface to the pool bottom J. Parameters J and J_p can be computed as follows:

$$J = \frac{D}{\sin\beta} \tag{8}$$

$$J_p = C_d^2 h_{\text{dpools}} \tag{9}$$

Here, $C_d = 2.6$; β is the angle between the jet impinging the pool and the horizontal plane; and $h_{\text{dpools}} = q_w/u_{\text{dpools}}$ is the jet thickness as it impinges into the pool where u_{dpools} is the velocity at the pool surface (Figure 3). The location where the jet impinges on the pool is assumed to be at the mid-length of the pool and the parameters u_{dpools}, D and β can be calculated with the drop height of the headcut H_{drop} and the velocity at the brink u_{dbrink} (Figure 3):

$$D = S_f u_{\text{dbrink}} \sqrt{\frac{2H_{\text{drop}}}{g}} \tag{10}$$

$$u_{\text{dpools}} = \frac{u_{\text{dbrink}}}{\cos\beta} \tag{11}$$

$$\beta = \arctan\frac{\sqrt{2gH_{\text{drop}}}}{u_{\text{dbrink}}} \tag{12}$$

The bottom velocity u_{dbottom} is then,

$$u_{\text{dbottom}} = \begin{cases} u_{\text{dpools}}, & J \le J_p \\ C_d\sqrt{\dfrac{h_{\text{dpools}}}{J}}\,u_{\text{dpools}} & J > J_p \end{cases} \tag{13}$$

Once q_w, $H_{\text{drop,}}$ and S_f are known, the shape of the plunge pool and the migration rate of the headcut can be obtained. And then the migration rate c_{sd} and velocity at the brink u_{brink} are introduced to predict the upstream region (using the Parker and Izumi (2000) model).

The plunge pool erodes when bottom shear stress τ_{bottom} exceeds the threshold value τ_{cr}. Expressions for the shear stress at the diffusion and nondiffusion states are:

Nondiffusion state

$$\tau_{\text{bottom}} = \rho C_{\text{fpool}}\left(2H_{\text{drop}}g + \frac{{q_w}^{2/3}g^{2/3}}{0.715^2}\right) \tag{14}$$

Diffusion state

$$\tau_{\text{bottom}} = \frac{0.715\rho C_d^2 C_{\text{fpool}} g^{2/3}}{S_f}{q_w}^{2/3} \tag{15}$$

We further define the upstream boundary of the pool as the intersection of the vertical headcut and the pool. With this definition, the bed elevation at this place is calculated as the difference between the bed elevation at the brink and the drop height H_{drop}. Based on the theory of Flores-Cervantes et al. (2006), at the upstream boundary of the pool the water surface level is equal to the bed elevation. Given that the bed elevation at the downstream end of the pool should be higher than the bed elevation at the center (i.e., the deepest point)

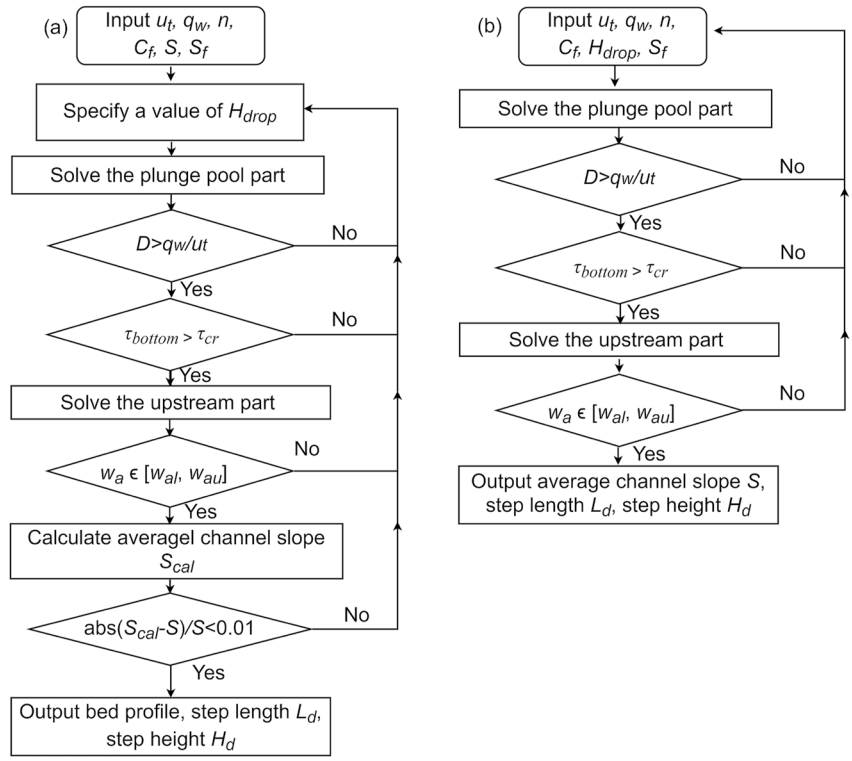

Figure 4. (a) Flow chart of the plunge pool model when the average channel slope S is known. (b) Flow chart of the plunge pool model when H_{drop} is known. In Figure 4a, S_{cal} denotes the average channel slope predicted by the model, and the input drop height H_{drop} is adjusted to make S_{cal} equal to S.

of the pool, we deduce that the depth of the pool should be larger than the flow depth at the end of the pool (i.e., the start point of next step). The flow field in the plunge pool is complex and multidimensional, but we can assume flow in the upstream region (just beyond the pool) is one dimensional. As such, we approximate the flow depth at $x_d = 0$ as q_w/u_t. Therefore, another condition for existence of the plunge pool is:

$$D \geq \frac{q_w}{u_t} \tag{16}$$

For a given set of parameters u_t, n, C_f, q_w, and S_f, there are two scenarios when implementing the plunge pool model. In the first scenario, we specify the average channel slope S, and the drop height of headcut H_{drop} is calculated through trial and error until the output average channel slope from the model S_{cal} equals our specified S (see the flow chart of calculation in Figure 4a). In the second scenario, H_{drop} is specified, and S is obtained explicitly (see the flow chart of calculation in Figure 4b). H_{drop} should obey the following conditions:

(1) the relation $\tau_{bottom} > \tau_{cr}$ should be satisfied;
(2) the relation $w_{al} < w_a < w_{au}$ should be satisfied in the Parker and Izumi (2000) model, where w_a is the dimensionless additional degradation rate calculated by subtracting the undercutting rate due to migration from the total undercutting rate; and w_{al} and w_{au} are the upper and lower bounds of w_a. Relations to calculate w_{al} and w_{au} are given in equation S10 of the Supporting Information S1. The relation $w_{al} < w_a < w_{au}$ is to allow the existence of the solution of the Parker and Izumi (2000) model, which is used to describe the domain upstream of the brink;
(3) we assume the water surface elevation in the pool equals the bed elevation at the upstream end of the pool, ensuring that the condition $D \geq q_w/u_t$ is satisfied.

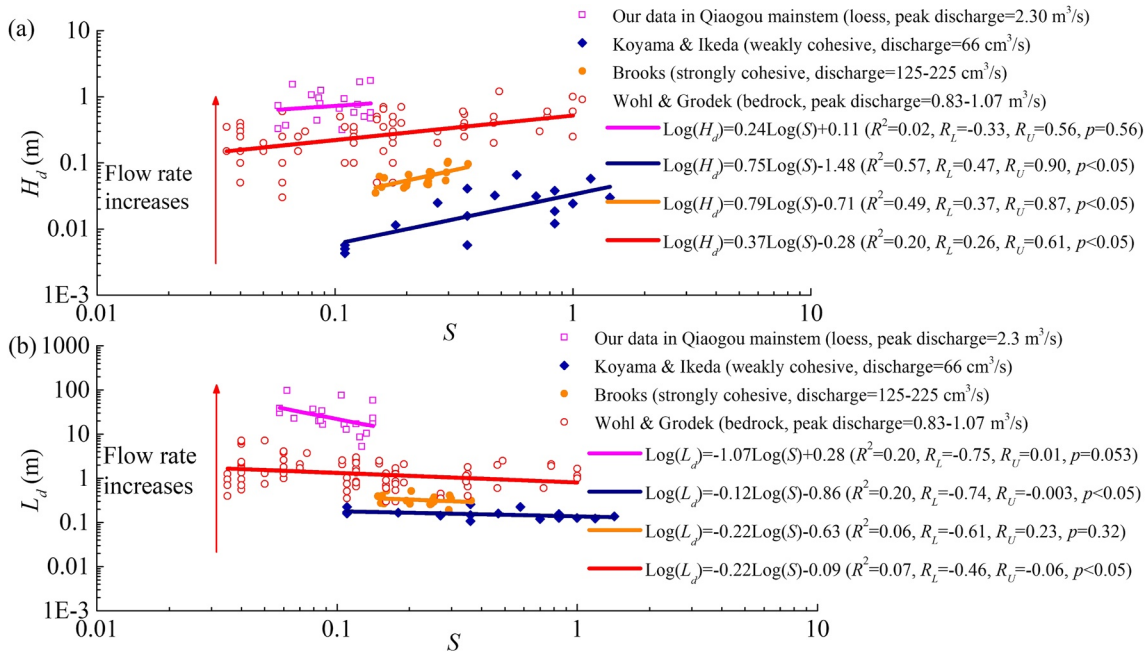

Figure 5. (a) Cyclic step height versus average channel slope for measured data. (b) Cyclic step length versus average channel slope for measured data. Field and laboratory data sets are separated using open points and solid points, respectively. R is the Pearson correlation coefficient; R_L and R_U are the 95% confidence bounds on the Pearson correlation coefficient; p value is significance level describing the probability computed assuming that the null hypothesis (i.e., the correlation between the variables exists) is true.

4. Observations From Measured Data

Cyclic step dimensions can be described in terms of step length and step height. Here, step length L_d is the horizontal distance between the deepest points of adjacent plunge pools, and step height H_d is the vertical distance from the bottom of the plunge pool to the brink of the headcut (Figure 3). To analyze the relations between cyclic step geometry and the channel variables, some channel variables must be extracted from measuring points. One important external indicator of step pool geometry is the average channel slope (Wohl et al., 1997). For each step in the Qiaogou mainstem, we calculate the average channel slope by linear regression of the longitudinal profile of a 200 m (approximately 7 times the average measured step length) section centered on the step. The average channel slope for other data sets in Table 1 is the average value over the entire channel or sub-channel, which is obtained from corresponding references.

Figure 5a plots step height versus average channel slope and Figure 5b plots step length versus average channel slope using different data sets of erosional cyclic steps. By comparing these two plots, we find that, as flow rate increases, L_d and H_d also increase. The difference in discharge may be the main factor that leads to the fact that all field data sets have higher values of L_d and H_d than laboratory data sets. All data sets, except for the Qiaogou mainstem, show a trend for increasing step height H_d as average channel slope S increases. The Koyama and Ikeda (1998) data set shows that step length slightly decreases as the average channel slope increases, while other data sets show no distinct trend between L_d and S based on the regression analyses.

The Qiaogou data set and bedrock data from Wohl and Grodek (1994) presented here conflate simultaneous trends for slope to decrease downstream and discharge to increase downstream via increased drainage area. These combined trends may explain why H_d and S exhibit no significant correlation in the data for the Loess Plateau. However, in bedrock data from Wohl and Grodek (1994) step height shows a positive correlation with slope. We infer that the effect of flow rate on step dimensions decreases as bed erodibility decreases. The coupling effects of flow rate and bed erodibility on cyclic step dimensions are discussed in the next section.

We define the step aspect ratio as step length over step height L_d/H_d, a dimensionless parameter, which is widely used in describing step pool geometry (Abrahams et al., 1995). With this dimensionless parameter, we can link steps in different environments and understand variations in cyclic step geometry. The average channel slope S here is a variable representing the characteristics of the entire reach or sub-reach, but L_d/H_d is a variable representing local changes (with a spatial scale about ~10 m in the Qiaogou mainstem) along the reach.

For step pools, the ratio L_d/H_d, which generally ranges from 5 to 16.7, has been found to be related to the average channel slope S (Abrahams et al., 1995). Abrahams et al. (1995) found that L_d/H_d falls in the range of $1/(2S) \le L_d/H_d \le 1/S$ for step-pools in both natural channels and flume experiments when the system achieves maximum stability (or maximum flow resistance). This is often rearranged as the relative steepness, which is the ratio of step slope to average channel slope $H_d/(L_dS)$, where unity (one) means the step slope and average bed slope are equal. Values greater than one imply the step relief is greater than the average slope and requires a negative slope gradient between steps. As $H_d/(L_dS)$ decreases, step height plays a diminishing role on the average channel slope and local slope between steps (or slope of the step's stoss face) increases.

Church and Zimmermann (2007) plotted the reach averaged $H_d/(L_dS)$ against S for data for natural step-pools, step-pools in flume experiments, and field drop structures, which are engineered step-like structures such as check dams and found that the relative steepness $H_d/(L_dS)$ is slope dependent. Due to the morphological similarity of cyclic steps and step pools, we compare cyclic step data to step pool data (via Church & Zimmermann, 2007) as shown in Figure 6a. The relative steepness $H_d/(L_dS)$ of alluvial cyclic steps is lower than step pools and bedrock cyclic steps have the largest relative steepness. Almost all alluvial cyclic steps have relative steepness below one, implying a lot of the relief occurs over the channel, whereas most of the values of $H_d/(L_dS)$ for concrete structures such as bedrock steps are above 1, implying that the step provides the main source of relief.

In Figure 6b, we study the relationship between the step aspect ratio L_d/H_d with the channel slope S. The step aspect ratio shows a decreasing trend with the increase of channel slope, which agrees with previous research of Brooks (2001). Golly et al. (2019) further demonstrated that for an ideally regular sequence of steps, L_d/H_d should be linearly related to S as a result of the geometry constraint; the variability of the steps, on the other hand, encompasses the process information and modulates the relation between L_d/H_d and S. From Figure 6b, we also observe difference in L_d/H_d among different bed material/lithologies, with larger L_d/H_d in weakly cohesive beds than steps in strongly cohesive beds or bedrock. We explore the effect of bed material on L_d/H_d in the following section using our model.

Comparisons of step aspect ratio to slope, as in Figure 6b, mask the influence of discharge on step formation as both directly influence the bed erosion rate. We note that the minimum average channel slopes with cyclic steps are smaller in the field than in laboratory experiments. We infer that this difference may be caused by the discharge magnitude, and, for a larger flow rate, steps can exist on a smaller slope. The influence of discharge on the minimum slope necessary to develop cyclic steps is explored by the new theory in the next section.

5. Model Performance

We test our new theory by comparing model results with observations from the measured data. As shown in Figure 7, the results of the new theory show that an increase in flow rate leads to a larger step length and step height, which is consistent with our observations from the measured data. Simulation results show that step dimensions become invariant to flow rate as bed erodibility decreases, as illustrated by the invariance of both L_d and H_d to discharge as threshold velocity increases (Figure 7).

Examples of the relationship between L_d and S and the relationship between H_d and S predicted by our new theory are shown in Figure 8. The figures show that our combined model can reproduce the trends for L_d and H_d with S in the measured data sets: step length L_d shows no distinct trend with slope step height H_d shows a positive trend with slope. Bed steps are seen to control almost all of the bed elevation drop in the channel when steps are accompanied by plunge pool erosion. As a result, step height has a strong positive

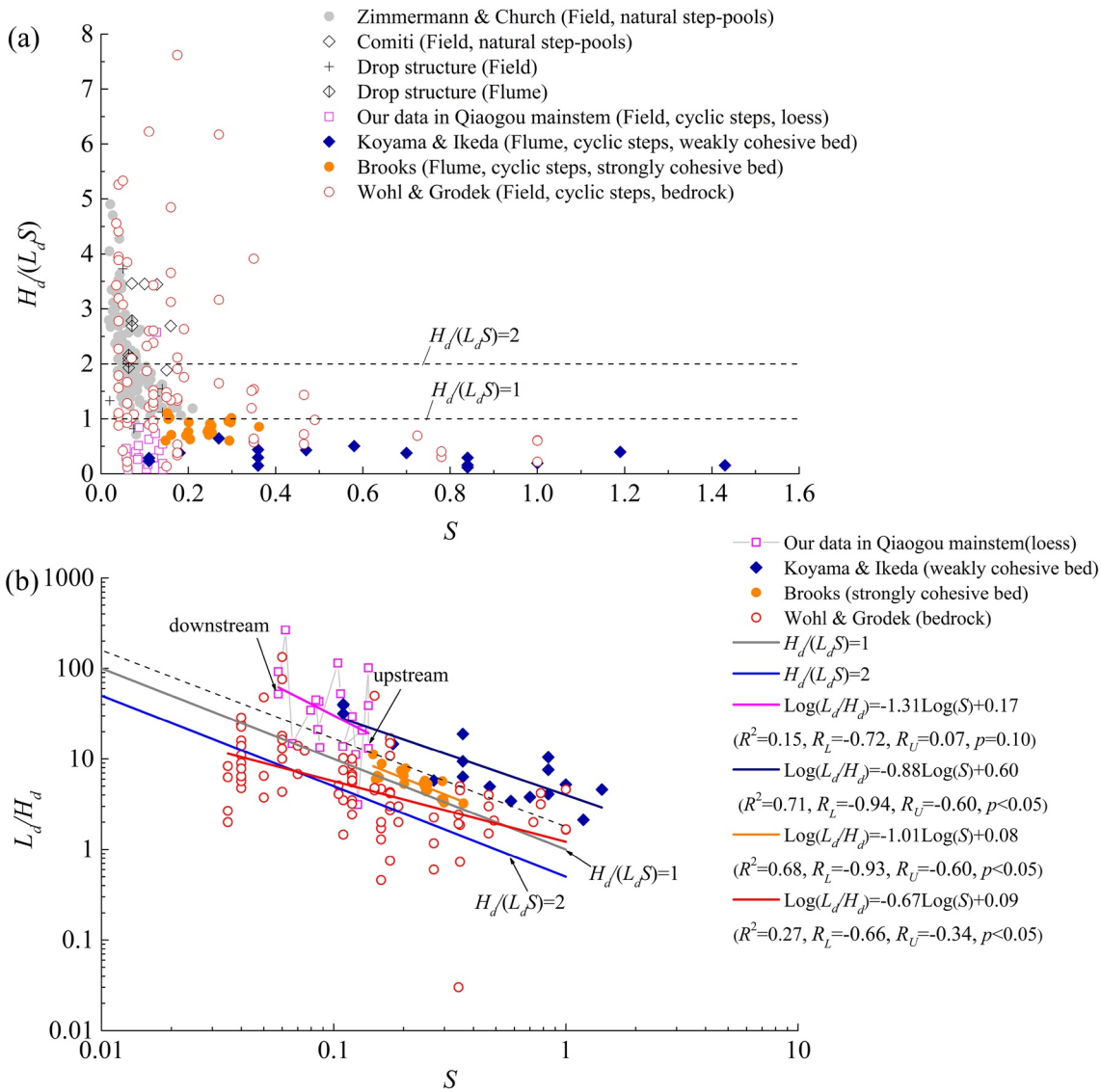

Figure 6. (a) Reach-averaged relative steepness $H_d/(L_dS)$ versus average channel slope S. Step pool data (Church & Zimmermann, 2007) is included with our compendium of erosional cyclic step measurements. The expected range of $H_d/(L_dS)$ for natural step-pool channels, which generally ranges from 1 to 2, is shown by the two dotted lines. (b) The cyclic step aspect ratio versus average channel slope. The expected range of $H_d/(L_dS)$ for natural step-pool channels, which generally ranges from 1 to 2, are drawn as red and blue lines, respectively. The black dotted line separates measurements from weakly cohesive beds from those of strongly cohesive bed and bedrock. Field and laboratory data sets for cyclic steps are separated into open points and solid points, respectively.

correlation with average channel slope. However, relative to step height, step length does not change as significantly with increased slope. This effect is expected as most of the step length exists upstream of the brink, in the region predicted by the Parker-Izumi model (2000). In our new theory, the bed profile upstream of the brink depends on two velocity boundary conditions and the retreat rate of the headcut. For a given discharge per width q_w, exponent n, and threshold velocity u_t, the length of the upstream section only depends on the retreat rate of the headcut. The conditions at the pool in Figure 8 correspond to the diffusion state, and, under this condition, the retreat rate is insensitive to the variability in drop height (Flores-Cervantes et al., 2006). Thus, the adjustment of step height with average channel slope does not cause a significant change in the migration rate, which reduces any change in step length as average channel slope increases. In addition, based on the results in Figure 8, the minimum slope that generates steps decreases as flow rate increases, which is consistent with our observations from the measured data.

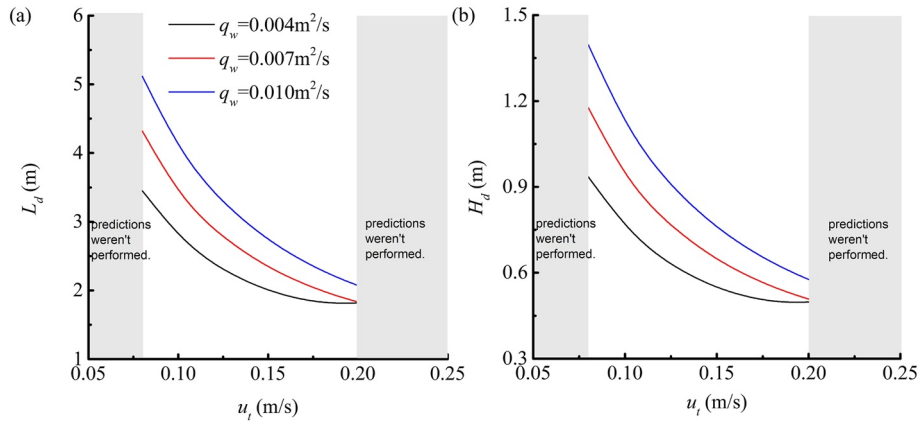

Figure 7. (a) Cyclic step length versus threshold velocity for different flow rates simulated with the plunge pool model. (b) Cyclic step height versus threshold velocity for different flow rates simulated with the plunge pool model. In these cases, the bed erosion exponent $n = 2$, the bed resistance coefficient upstream of the headcut $C_f = 0.01$, and the average channel slope $S = 0.25$; the shape factor S_f is 0.5 in the plunge pool model; the lines end because the theoretical predictions were not performed.

Furthermore, we use the new theory to make a direct comparison with observed L_d and H_d in the experiments of Brooks (2001). Here, we choose the data sets of Brooks (2001) instead of Koyama and Ikeda (1998) to test the validity of the theory because Brooks' experimental data are more suitable for determining model parameters and do not include the influence of lateral erosion. In these experiments, the bed resistance coefficient C_f and discharge per width q_w are known but the threshold velocity u_t, exponent n, and shape factor S_f are difficult to measure. The threshold velocity u_t is influenced by several vagaries of cohesive soil such as time of drying, and thus it is different in each experimental run due to the variation in soil drying time. Threshold velocity u_t must be smaller than the normal flow velocity in the absence of steps measured in the experiments of Brooks (2001), which gives an upper bound of u_t. According to the measured data, S_f is not a constant and the range of S_f is determined via measured S_f (Table S5 of the Supporting Information S1). The range of n is from 1 to 4. By adjusting u_t, n, and S_f in each run, step length and step height in the experiments can be predicted. The comparison between observed and predicted step length and step height is shown in

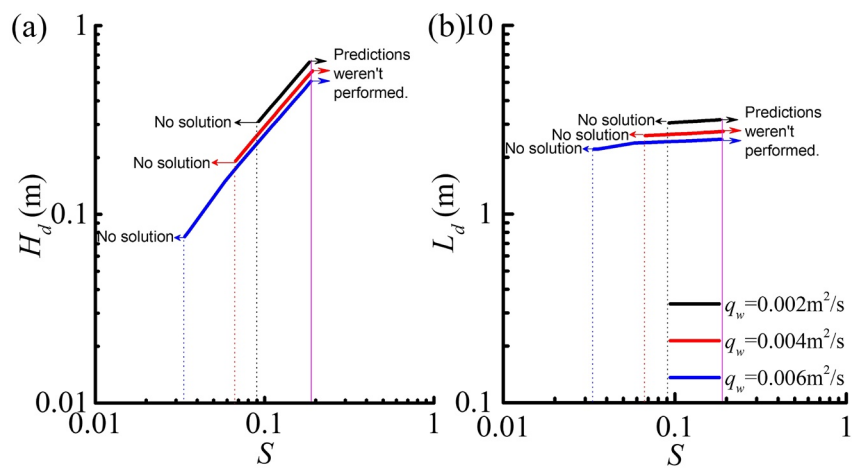

Figure 8. (a) Cyclic step height versus average channel slope for different flow rates simulated with the plunge pool model. (b) Cyclic step length versus average channel slope for different flow rates simulated with the plunge pool model. In these cases, the bed erosiont exponent $n = 2$, the threshold velocity for bed erosion upstream of the headcut $u_t = 0.1$ m/s, the bed resistance coefficient upstream of the headcut $C_f = 0.01$, and the shape factor S_f is 0.5 in the plunge pool model; the lines end on the left because there is no solution, and end on the right because the predictions were not performed.

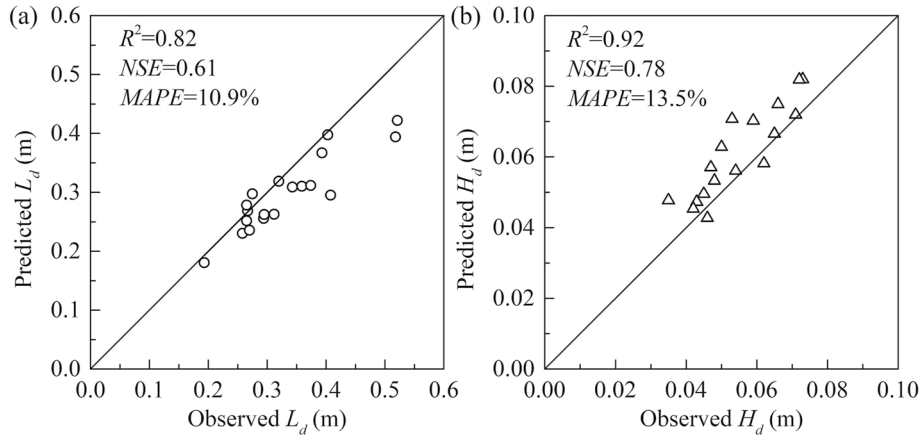

Figure 9. Step dimensions for length L_d and height H_d via Brooks (2001) experiments are compared to results of the combined model. (a) Observed versus predicted step length (b) Observed versus predicted step height. We use the coefficient of determination R^2, Nash-Sutcliffe efficiency coefficient *NSE,* and mean-absolute percentage error *MAPE* as goodness-of-fit statistics.

Figure 9 and Table S6 in Supporting Information S1 presents parameters of the theory, observed values of dimensional step length and step height, and computed ones.

The new model predicts the trend for decreasing L_d/H_d as the average channel slope increases (Figure 10). Based on the previous analysis, a larger slope is accompanied by a larger step height. Thus, at a given value of S_f, the step aspect ratio L_d/H_d decreases as the drop height of the headcut H_{drop} increases (Figure 11). The bed slope upstream of the brink increases as H_{drop} increases and can be positive, negative, or nearly horizontal (Figure 11). As such, L_d/H_d is not necessarily equal to S^{-1}.

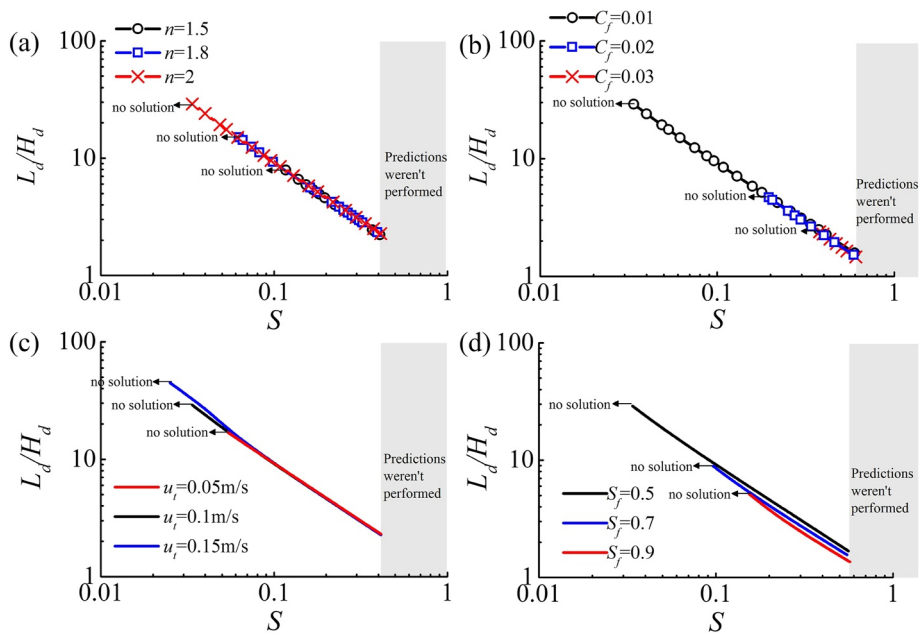

Figure 10. (a) Cyclic step aspect ratio L_d/H_d versus average channel slope simulated with the plunge pool model. Different diagrams explore the sensitivity to: (a) erosion rate exponent n ($C_f = 0.01$, $u_t = 0.1$ m/s, $q_w = 0.002$ m^2/s, $S_f = 0.5$), (b) bed resistance coefficient C_f ($n = 2$, $u_t = 0.1$ m/s, $q_w = 0.002$ m^2/s, $S_f = 0.5$), (c) threshold velocity u_t ($n = 2$, $q_w = 0.002$ m^2/s, $S_f = 0.5$, $C_f = 0.01$), and (d) shape factor S_f ($n = 2$, $q_w = 0.002$ m^2/s, $C_f = 0.01$, $u_t = 0.1$ m/s). The lines end on the left because there is no solution and end on the right because the calculations were not performed.

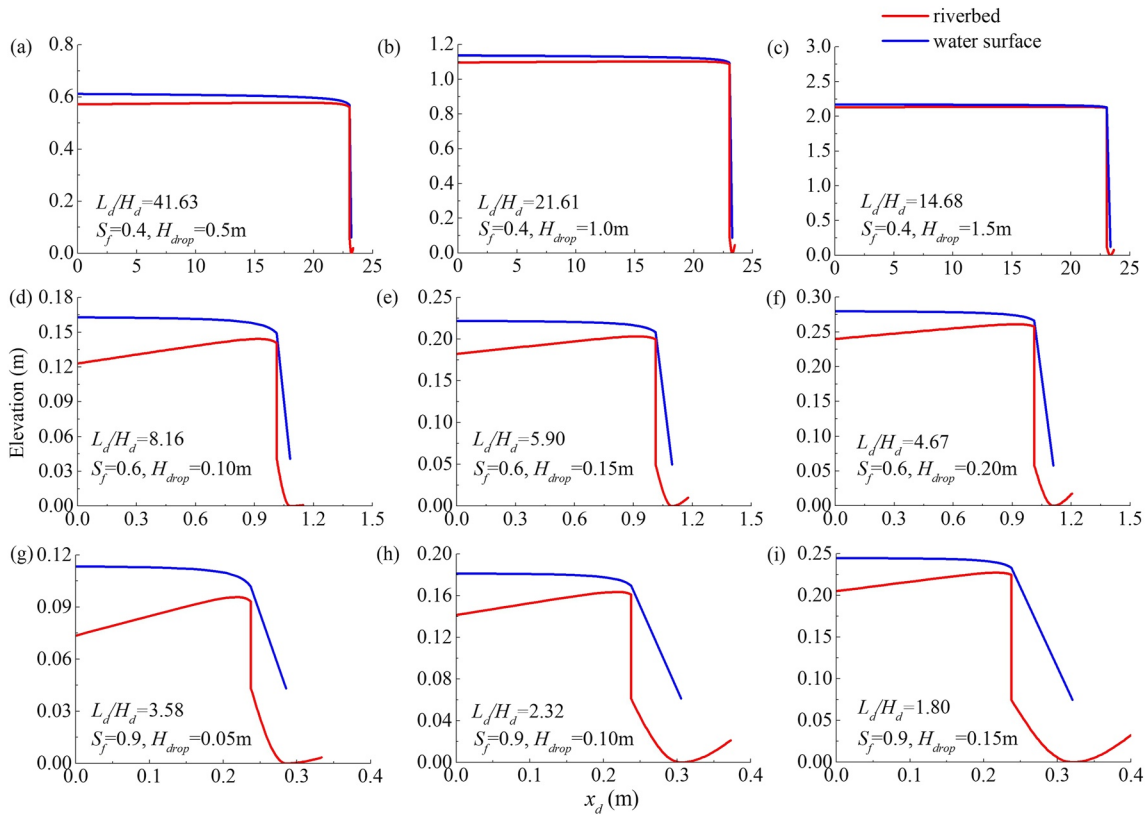

Figure 11. Bed levels and water surface levels predicted by the plunge pool model. ($C_f = 0.01$, $n = 2$, $q_w = 0.004$ m^2/s, and $u_t = 0.1$ m/s). Values of L_d/H_d, S_f, and H_{drop} vary across the subplots, with the values given in each panel of the figure separately.

We consider whether the step aspect ratio L_d/H_d, depends on bed erodibility through a sensitivity analysis. Erosion rate exponent n and threshold velocity u_t hardly affect the step aspect ratio L_d/H_d, although there is a slightly increasing trend between L_d/H_d and u_t (Figure 10c). The effect of the bed resistance coefficient upstream of the brink C_f on step aspect ratio L_d/H_d is minor (Figure 10b).

We analyze the shape factor in the Qiaogou watershed, Brook's experiments, and bedrock channels (Tables S5, S7 and S8 of the Supporting Information S1) and find that S_f is not consistently equal to 0.5, that is, the value that has been used in our previous simulations with the plunge pool model. Compared to other parameters, the step aspect ratio L_d/H_d is sensitive to the shape factor S_f, and as the shape factor S_f increases, the minimum bed slope that generates steps must also increase (Figure 10d). Therefore, the observed trend for decreasing L_d/H_d as bed erodibility decreases may be caused by the difference in S_f for various bed materials (average S_f in strongly cohesive beds and bedrock are larger than that of weakly cohesive bed in the Loess Plateau, as shown in Tables S5, S7, and S8 of the Supporting Information S1). Figure 11 presents bed profiles predicted by the new theory with varying S_f. The simulations show that as the shape factor S_f increases, both step height and step length decrease (more evidence can be found in Figure S10 of the Supporting Information S1). Furthermore, the ratio of plunge pool length to the entire step length increases with increasing S_f (Figure 11).

Based on the previous analyses in Figure 10, we conclude that the shape factor S_f is the major factor that affects the step aspect ratio L_d/H_d at a given average channel slope S. This is consistent with the conclusion of Comiti et al. (2005), who found that L_d/H_d in step-pool systems are controlled by the shape factor for pools and the average channel slope.

In Figure 12, we compute results assuming a range for each parameter of the model ($C_f \in [0.01, 0.05]$, $u_t \in [0.1$ m/s, 0.9 m/s$]$, $S_f \in [0.1, 0.9]$, $q_w \in [0.001$ m^2/s, 5 m^2/s$]$, and $n \in [1.5, 4]$) instead of just three values for each parameter as shown in Figure 10 to understand the range of L_d/H_d that the model can predict. All the

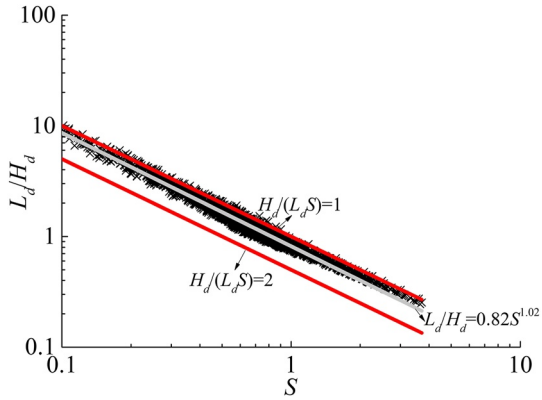

Figure 12. Cyclic step aspect ratio from about 3,000 numerical runs of the plunge pool model (The range of simulation parameters is $C_f \in [0.01, 0.05]$, $u_t \in [0.1\ m/s, 0.9\ m/s]$, $S_f \in [0.1, 0.9]$, $q_w \in [0.001\ m^2/s, 5\ m^2/s]$, and $n \in [1.5, 4]$). The expected range of $H_d/(L_dS)$ from 1 to 2 for natural step pools is shown by the two red lines. The gray line is a curve fitted to the numerical data with a power function.

points $(S, L_d/H_d)$ of the simulations fall between the lines of $H_d/(L_dS) = 1$ and $H_d/(L_dS) = 2$. A power-law regression between L_d/H_d and S for the numerical data (the gray line in Figure 12) gives an exponent near −1. In this case, each step has a vertical headcut and most of the total drop in bed elevation over the entire step length is contributed by the height of the headcut plus the depth of the plunge pool. Thus, L_d/H_d is approximately equal to S^{-1}. At a given average channel slope S, adjusting the parameters in the new theory leads to a narrow range of L_d/H_d (Figure 12).

The added mechanism of plunge pool erosion is not sufficient to explain the range of L_d/H_d in the measured data. One possible reason is that the model fails to consider the transient development of cyclic steps. As we state in Section 2.2, the steps in the Qiaogou watershed are in a transient state rather than in equilibrium. For the Qiaogou data, there are large fluctuations in the values of L_d/H_d from upstream to downstream (Figure 5b). The upstream steps are older and assumably closer to an equilibrium state, however, this upward migration also implies increased average channel slope and decreased discharge, which also affect step shape. The present model is unable to account for all these factors at this time.

By comparison, we also conduct numerical simulations using the Parker and Izumi (2000) model. The results of the Parker and Izumi (2000) model show that a lower bed erodibility leads to a smaller step aspect ratio. However, the Parker and Izumi (2000) model is unable to predict the range of L_d/H_d in the measured data by adjusting the parameters in the model. The trend between H_d and S and the trend between L_d and S in the measured data cannot be predicted by the Parker and Izumi (2000) model. For more details about the analyses of the Parker and Izumi (2000) model, readers are referred to Text S2 of the Supporting Information S1.

6. Discussion

6.1. Limitations and Simplifications of the Plunge Pool Model

Lateral erosion driven by radial turbulent jets toward the pool sidewalls is not accurately calculated in the model. We roughly estimate the lateral erosion rate at the headcut by dividing vertical erosion rate by a shape factor. Here, the model assumes that the deepest point of the pool is at the center of the pool domain and the shape factor (i.e., the pool depth divided by half the pool length) is a constant determined only by the type of bed material. Our results show that step geometry is sensitive to the value of this shape factor.

Plunge pool size has been evaluated for non-cohesive beds (Pagliara et al., 2006) and in bedrock (Scheingross & Lamb, 2016), but not yet in cohesive beds, as in the Loess Plateau. In the future, development of a theory capable of estimating the shape factor for cohesive beds would improve the accuracy of our model. Furthermore, the Flores-Cervantes et al. (2006) model assumes that the impinging point of the jet is at the center of the pool. Some laboratory experiments show steps are self-affine and the longitudinal location of the maximum depth is at the center of the pool (Comiti, 2003). However, plunge pool experiments in bedrock have shown that lateral erosion is not spatially uniform and is concentrated on the downstream sidewall of the pool instead (Scheingross et al., 2017). In non-cohesive beds, the scour hole profile is almost symmetrical when the jet impact angle is 90° (Pagliara et al., 2006). Yet, the jet impact angles from 30° to 60° would develop an asymmetric plunge pool profile with the deepest point further downstream from the pool center (Pagliara et al., 2006). Future research that better parametrizes pool geometry and development will improve results of our model as well.

We assume that the threshold velocity for bed erosion is achieved at the upstream end of a step. If the velocity at the upstream end exceeds the threshold velocity, erosion of the pool sidewall would continue, expanding the pool length. This effect would continue until the velocity reduces to the threshold velocity at the pool edge. The model is unable to develop solutions for cyclic steps in this case. Alternatively, if velocity at $x_d = 0$ is less than the threshold value, another zone will develop characterized by flow acceleration toward threshold velocity and no bed erosion as well as migration rate. However, this acceleration zone cannot

exist in steady solutions of cyclic steps because the whole step would migrate upstream at a constant rate and this zone will be reduced to disappear. Therefore, as we are more interested in equilibrium features, it is reasonable to assume the flow velocity at the upstream boundary must be equal to the threshold velocity.

According to Comiti et al. (2005), the flow tends to remain critical in natural steep streams and thus it is reasonable to assume critical flow ($F_r = 1$) at the brink. The flow accelerates from the end of a pool to the next downstream brink. Based on the arguments in Comiti et al. (2005), the flow upstream of the brink is subcritical ($F_r < 1$). For simplicity, we estimate the flow depth and velocity at the brink using the relations corresponding to the subcritical regime in the model of Flores-Cervantes et al. (2006).

In the model of Flores-Cervantes et al. (2006), pool depth only depends on discharge, drop height, and shape factor. Stein et al. (1993) proposed a formula for equilibrium pool depth applicable to any jet configuration and bed material. In their theory, equilibrium scour depth is met when the maximum shear stress at the pool bottom is equal to the critical shear stress for the bed material. The equilibrium pool depth in Stein et al.'s theory can be expressed as:

$$D_e = \frac{C_d^2 \rho C_{\text{fpool}} u_{\text{dpools}}^2 h_{\text{dpools}}}{\tau_{cr}} \sin \beta \tag{17}$$

we remind the reader that u_{dpools} and h_{dpools} are the jet velocity and jet thickness at the pool surface, respectively, $C_d = 2.6$ is the diffusion coefficient, τ_{cr} is the critical shear stress for the bed material, C_{fpool} is the bed resistance coefficient in the pool region, and β is the impinging angle.

Via this theory, the equilibrium pool depth is set when the bottom can no longer erode the bed sediment, making the vertical undercutting rate of the plunge pool $dD/dt = 0$. According to Equation 4 in this paper, the migration rate of the headcut is zero when $dD/dt = 0$ (i.e., $D = D_e$). We compare D_e from the theory of Stein et al. (1993) with D from the theory of Flores-Cervantes et al. (2006), under the same drop height H_{drop} and discharge q_w. The results show that there is a large difference between D_e and D (Figure S11 of the Supporting Information S1), indicating that cyclic steps migrate upstream in most cases because dD/dt is not equal to 0 when $D_e \neq D$.

The adopted theory for plunge pool erosion may not include all the salient variables to accurately model their formation. For example, maximum depth of plunge pool scour is also influenced by the densimetric Froude number, jet air entrainment, the tailwater downstream of the pool, and sediment nonuniformity in non-cohesive scour holes (Pagliara et al., 2006). Sediment supply, which is completely omitted in our study, is also considered a key predictor for erosion of bedrock plunge pools (Scheingross & Lamb, 2016). Additionally, the equilibrium theories for pool depth we discussed here (including Stein et al., 1993; Pagliara et al., 2006; Scheingross & Lamb, 2016) necessarily imply a solitary step or single headcut of permanent form, rather than cyclic or periodic steps that migrate upstream.

6.2. The Potential Physics That Control Cyclic Step Geometry

Some theories for steps in step-pool systems have been proposed to predict geometric features. Wohl and Grodek (1994) proposed that channel slope controls the spacing of flow structures. They offered, however, no verification using flume experiments. Judd (1963) and Judd and Peterson (1969) proposed that step length is closely related to standing wave characteristics, whereas Allen (1982, 1983) suggested that hydraulic jumps are an important mechanism for step formation. Comiti et al. (2005) found that step spacing is controlled by jet energy, which supported the theory of Judd (1963) and Judd and Peterson (1969). Moreover, the "jammed state" hypothesis is used to explain the formation of depositional steps in step-pool channels and the formation of steps is enhanced by rough banks and width variations (Church & Zimmermann, 2007; Saletti & Hassan, 2020; Zimmermann et al., 2010).

Similar to step pools, hydraulics jumps are understood to be essential for cyclic step formation and stabilization in homogeneous beds. Due to the importance of hydraulic jumps, the model developed by Allen (1982, 1983), which suggested the importance of hydraulic jumps in step-pool formation, can provide an opportunity to explain the characteristics of cyclic steps. However, the role of hydraulic jumps on step formation is different between step pools and cyclic steps. For step-pools, hydraulic jumps control

the accumulation of large particles, and thereby determine the locations of steps downstream (Allen, 1982, 1983). For cyclic steps, hydraulic jumps result in energy dissipation and unequal bed slopes (lee slope vs. stoss slope) via transitions between subcritical and supercritical flow along the channel, which lead to the formation of new steps downstream (Fagherazzi & Sun, 2003). Therefore, it may be possible to explain the morphological characteristics of cyclic steps from the perspective of energy dissipation caused by hydraulic jumps.

The trends for step length and step height with increased average channel slope are different between the Parker and Izumi (2000) model and our new theory. One possible explanation is that the patterns of energy dissipation are different in the two cases. In the Parker and Izumi (2000) model, the head loss is mainly controlled by alternating internal hydraulic jumps. For a given bed erodibility and flow discharge, the head loss at each hydraulic jump is fixed. The steps adjust the energy slope by adjusting step length at a given average channel slope. To keep pace with step length so as to obtain a specified average channel slope, step height must also adjust.

In the plunge pool model, energy dissipation is mainly caused by turbulent mixing in the pool domain. In order to analyze the relation between the adjustment of cyclic step geometry and the energy dissipation in the plunge pool model, the energy dissipation in the plunge pool domain is calculated using Equation 18, which is the general energy equation considering jump submergence for natural mountain channels (Pasternack et al., 2006; Wilcox et al., 2011; Wyrick & Pasternack, 2008). The energy equation between the section at the brink and the section just downstream of the pool can be expressed as follows:

$$\eta_{\mathrm{dbrink}} + h_{\mathrm{dbrink}} + \frac{\alpha_2 u_{\mathrm{dbrink}}^2}{2g} = \eta_{\mathrm{dpoolend}} + h_{\mathrm{dpoolend}} + \frac{\alpha_2 u_{\mathrm{dpoolend}}^2}{2g} + h_L \tag{18}$$

where the subscripts "brink" and "poolend" refer to locations at the brink and at the downstream end of the pool, respectively; α_2 is a kinetic energy correction factor that represents the degree of variation in velocity across a section; and h_L is head loss (Figure 1c). Here, u_{dbrink} depends on flow discharge and u_{dpoolend} is assumed to be approximately equal to the threshold velocity for bed erosion. The energy coefficient α_2 in Equation (18) is assumed to be the same at the upstream and downstream sections. The flow condition is assumed to be steady and the pressure head can be taken as hydrostatic. The water-surface slope is low, so that the flow depth measured normal to the water surface can be approximated by the vertical distance below the water surface. Furthermore, we assume that the upstream total energy and the downstream tailwater depth are independently controllable. For a given discharge and bed erodibility, the head loss caused by the change in flow depth and flow velocity is fixed. And in this case, the head loss depends on the bed elevation difference between the brink and the pool end (η_{dbrink}–η_{dpoolend}), which is in turn equal to step height minus the water depth at the pool end (Figure 3). In the plunge pool model, steps adjust energy dissipation by adjusting step height, rather than step length as in the Parker and Izumi (2000) model. The adjustment of step height can further lead to the change in step length in the following way. According to Equations 5–13, the adjustment in step height influences drop height H_{drop} and then change the vertical erosion rate of the plunge pool dD/dt. The change in dD/dt further leads to the variation in the migration rate (shown in Equation 4). The migration rate eventually influences the length upstream the brink, and thus the total step length.

7. Conclusions

Cyclic steps are widespread in upland steep channels. These steps are often characterized by eroding plunge pools. However, the manner in which cyclic steps are controlled by a combination of both fluvial erosion driven by bed shear stress and plunge pool erosion is still unclear. In this study, we provide a large-scale comparison of field and laboratory measurements of subaerial cyclic steps formed in weakly and strong cohesive sediments as well as bedrock to theoretical predictions, using a new theory considering plunge pool erosion. The main contributions include: (a) The geometric features and controlling physics of erosional cyclic steps are identified using measured data and theoretical analysis; (b) We develop a new theory of erosional steps considering plunge pool erosion that can explain the observations on cyclic step morphology. The salient conclusions of our study are listed below:

1. Measured data sets indicate that step length L_d shows no significant relationship with the average channel slope S, and that cyclic step height H_d increases with an increasing average channel slope S. As flow rate q_w increases, step length L_d and step height H_d increase.
2. Measured data sets indicate that cyclic step aspect ratio L_d/H_d decreases with channel average slope S and increases as bed erodibility increases.
3. The new model developed herein can reproduce the observations from the measured data sets. However, it is not able to predict the scatter of L_d/H_d exhibited by the measured data. One possible reason is that the model does not consider the transient adjustment of step geometry ongoing with time.

Nomenclature

Cd	Diffusion coefficient (= 2.6), [1].
C_f	Dimensionless bed resistance coefficient for the region where erosion is caused by bed shear stress acting over the length of the bed, [1].
C_{fpool}	Dimensionless bed resistance coefficient for the region where erosion is caused by local plunge pool processes, [1].
c_{sd}	Dimensional migration rate of the headcut, [LT^{-1}].
D	Pool depth, [L].
D_e	Equilibrium pool depth, [L].
g	Gravitational acceleration (= 9.81 m/s^2), [LT^{-2}].
E	Erosion rate, [LT^{-1}].
H_d	Step height, [L].
$H_d/(L_dS)$	Relative steepness, [1].
H_{drop}	Drop height of the waterfall, [L].
h_L	Head loss over the length of a step, [L].
h_{dbrink}	Dimensional flow depth at the brink of the headcut, [L].
h_{dpoolend}	Dimensional flow depth at the end of the plunge pool, [L].
h_{dpools}	Thickness of the jet as it impinges on the pool, [L].
J	Distance from the impinging point at the pool surface to the impinging point at the pool bottom, [L].
J_p	Threshold distance at which no diffusion of the centerline velocity occurs in the pool domain, [L].
L_d	Step length, [L].
L_d/H_d	Step aspect ratio, [1].
n	Exponent in the relation for bed erosion, [1].
q_w	Dimensional flow rate per width, [L^2T^{-1}].
S	Average bed slope, [1].
S_{cal}	The average channel slope predicted by the model, [1].
S_f	Shape factor of the plunge pool, [1].
t	Dimensional time, [T].
u_d	Depth-averaged velocity, [LT^{-1}].
u_t	Dimensional threshold velocity for bed erosion in the upstream of the brink, [LT^{-1}].
u_{tpool}	Threshold velocity for bed erosion in the pool region, [LT^{-1}].
u_{dbrink}	Dimensional velocity at the brink of the headcut, [LT^{-1}].
u_{dbottom}	Flow velocity at the bottom of the pool, [LT^{-1}].
u_{dpoolend}	Dimensional velocity at the end of the plunge pool, [LT^{-1}].
u_{dpools}	Dimensional velocity at the surface of the plunge pool, [LT^{-1}].
w_a	Dimensionless undercutting rate in addition to that caused by horizontal migration, [1].
w_{al}	Lower bound on w_a, [1].
w_{au}	Upper bound on w_a, [1].
X_{m}	Half-length of plunge pool, [L].
α	Constant coefficient in the relation for bed erosion, [1].
α_1	Constant coefficient in the relation for plunge pool erosion, [1].
α_2	Kinetic energy correction factor in Bernoulli equation, [1].

β	Angle between the jet impinging on the pool and the horizontal plane, [1].
ρ	Flow density (= 1,000 kg/m^3), [ML^{-3}].
ν	Kinematic viscosity of water (= 10^{-6} m^2/s), [L^{2}T^{-1}].
η_{dbrink}	Dimensional bed elevation at the brink of the headcut, [L].
η_{dpoolend}	Dimensional bed elevation at the end of the plunge pool, [L].
τ_{cr}	Threshold bed shear stress for bed erosion, [ML^{-1}T^{-2}].
τ_{bottom}	Bed shear stress at the bottom of the pool, [ML^{-1}T^{-2}].

Data Availability Statement

Laboratory and field data sets of erosional cyclic steps and model simulation results used for this research can be found at http://doi.org/10.5281/zenodo.4317028. The data sets of step-pools used for this research are included in the paper in Church and Zimmermann (2007). Supplementary texts, figures, tables, and model codes can be found in the Supporting Information S1.

Acknowledgments
The authors gratefully acknowledge the support of the National Natural Science Foundation of China (51525901, 41941019, and 52009063) and the National Key Research and Development Program of China (2016YFC0402406). Gary Parker gratefully acknowledges US National Science Foundation for support through Division of Earth Science (EAR) Grant 1427262. The Authors wish to thank Xingyu Chen, Bingjie Wang, and Yi Liu for their help in carrying out the field survey in the Loess Plateau. Ellen E. Wohl and Peter C. Brooks are acknowledged for providing measured data sets of erosional steps. We thank the editor Mikael Attal, the reviewer Joel Scheingross, and two other anonymous reviewers for their constructive comments and remarks, which helped us greatly improve the manuscript.

References

Abrahams, A. D., Li, G., & Atkinson, J. F. (1995). Step-pool streams: Adjustment to maximum flow resistance. *Water Resources Research*, *31*(10), 2593–2602. https://doi.org/10.1029/95WR01957

Allen, J. R. L. (1982). *Sedimentary structures: Their character and physical basis*. Elsevier Scientific Pub. Co.

Allen, J. R. L. (1983). A simplified cascade model for transverse stone-ribs in gravelly streams. *Proceedings of the Royal Society of London: Mathematical*, *385*, 253–266. https://doi.org/10.1098/rspa.1983.0014

Alonso, C. V., Bennett, S. J., & Stein, O. R. (2002). Predicting head cut erosion and migration in concentrated flows typical of upland areas. *Water Resources Research*, *38*(12), 39-1–39-15. https://doi.org/10.1029/2001WR001173

Ashida, K., & Sawai, K. (1977). *A Study on the Stream Formation Process on a Bare Slope (3): Three Dimensional Channel Form, Annuals* (Vol. 20, pp. 1–15). Disaster Prevention Research Institute, Kyoto University. (In Japanese).

Balmforth, N. J., & Vakil, A. (2012). Cyclic steps and roll waves in shallow water flow over an erodible bed. *Journal of Fluid Mechanics*, *695*, 35–62. https://doi.org/10.1017/jfm.2011.555

Brooks, P. C. (2001). *Experimental study of erosional cyclic steps*. (p. 30). PhD Thesis, University of Minnesota.

Cheng, X. (2019). *5-Subchannel Analysis for LMR, Thermal Hydraulics Aspects of Liquid Metal Cooled Nuclear Reactors* (pp. 185–211).

Chin, A., & Wohl, E. (2005). Toward a theory for step pool in stream channels. *Progress in Physical Geography*, *29*(3), 275–296. https://doi.org/10.1191/0309133305pp449ra

Church, M., & Zimmermann, A. (2007). Form and stability of step-pool channels: Research progress. *Water Resources Research*, *43*, W03415. https://doi.org/10.1029/2006WR005037

Comiti, F. (2003). *Local scouring in natural and artificial step pool systems*. PhD Thesis (p. 209). Università degli Studi di Padova.

Comiti, F., Andreoli, A., & Lenzi, M. A. (2005). Morphological effects of local scouring in step–pool streams. *Earth Surface Processes and Landforms: The Journal of the British Geomorphological Research Group*, *30*(12), 1567–1581. https://doi.org/10.1002/esp.1217

Curran, J. C. (2007). Step-pool formation models and associated step spacing. *Earth Surface Processes and Landforms*, *32*(11), 1611–1627. https://doi.org/10.1002/esp.1589

Curran, J. C., & Wilcock, P. R. (2005). Effect of sand supply on transport rates in a gravel-bed channel. *Journal of Hydraulic Engineering*, *131*(11), 961–967. https://doi.org/10.1061/(asce)0733-9429(2005)131:11(961)

Fagherazzi, S., & Sun, T. (2003). Numerical simulations of transportational cyclic steps. *Computers & Geosciences*, *29*(9), 1143–1154. https://doi.org/10.1016/S0098-3004(03)00133-X

Fildani, A., Normark, W. R., Kostic, S., & Parker, G. (2006). Channel formation by flow stripping: Large-scale scour features along the Monterey East Channel and their relation to sediment waves. *Sedimentology*, *53*(6), 1265–1287. https://doi.org/10.1111/j.1365-3091.2006.00812.x

Flores-Cervantes, J. H., Istanbulluoglu, E., & Bras, R. L. (2006). Development of gullies on the landscape: A model of headcut retreat resulting from plunge pool erosion. *Journal of Geophysical Research: Earth Surface*, *111*, F01010. https://doi.org/10.1029/2004JF000226

Golly, A., Turowski, J. M., Badoux, A., & Hovius, N. (2019). Testing models of step formation against observations of channel steps in a steep mountain stream. *Earth Surface Processes and Landforms*, *44*(1), 1390–1406. https://doi.org/10.1002/esp.4582

Grant, G. E. (1994). *Hydraulics and sediment transport dynamics controlling step-pool formation in high gradient streams: A flume experiment, dynamics and geomorphology of mountain rivers*. Springer Berlin Heidelberg.

Grimaud, J. L., Paola, C., & Voller, V. (2016). Experimental migration of knickpoints: Influence of style of base-level fall and bed lithology. *Earth Surface Dynamics*, *4*(1), 11–23. https://doi.org/10.5194/esurf-4-11-2016

Izumi, N., Yokokawa, M., & Parker, G. (2017). Incisional cyclic steps of permanent form in mixed bedrock-alluvial rivers. *Journal of Geophysical Research: Earth Surface*, *122*(1), 130–152. https://doi.org/10.1002/2016JF003847

Judd, H. E. (1963). *A study of bed characteristics in relation to flow in rough, high-gradient natural channels, PhD dissertation*. Utah State University.

Judd, H. E., & Peterson, D. F. (1969). *Hydraulics of Large Bed Element Channels, Report PRWG* (Vol. 17–6). Utah Water Research Laboratory.

Kostic, S., & Parker, G. (2006). The response of turbidity currents to a canyon-fan transition: Internal hydraulic jumps and depositional signatures. *Journal of Hydraulic Research*, *44*(5), 631–653. https://doi.org/10.1080/00221686.2006.9521713

Kostic, S., Sequeiros, O., Spinewine, B., & Parker, G. (2010). Cyclic steps: A phenomenon of supercritical shallow flow from the high mountains to the bottom of the ocean. *Journal of Hydro-Environment Research*, *3*(4), 167–172. https://doi.org/10.1016/j.jher.2009.10.002

Koyama, T., & Ikeda, H. (1998). *Effect of Riverbed Gradient on Bedrock Channel Configuration: A Flume Experiment. Proc. Environmental Research Center*. (Vol. 23, pp. 25–34). Tsukuba University. (In Japanese).

Lamb, M. P., Howard, A. D., Dietrich, W. E., & Perron, J. T. (2007). Formation of amphitheater-headed valleys by waterfall erosion after large-scale slumping on Hawai'i. *Geological Society of America Bulletin*, *119*(7–8), 805–822. https://doi.org/10.1130/b25986.1

Lohnes, R. A., & Handy, R. L. (1968). Slope angles in friable loess. *Journal of Geology*, *76*(3), 247–258. https://doi.org/10.1086/627327
Luo, Y. H. (2015). *Analysis of characteristics loess orthostatic and applications*. Master's thesis (p. 56). Changan University.
Pagliara, S., Hager, W. H., & Minor, H. E. (2006). Hydraulics of plane plunge pool scour. *Journal of Hydraulic Engineering*, *132*(5), 450–461. https://doi.org/10.1061/(asce)0733-9429(2006)132:5(450)
Parker, G. (1996). Some speculations on the relation between channel morphology and channel-scale flow structures. In P. Ashworth, S. J. Bennett, J. L. Best, & S. J. McLelland (Eds.), *Coherent flow structures in open channels* (pp. 429–432). Wiley.
Parker, G., & Izumi, N. (2000). Purely erosional cyclic and solitary steps created by flow over a cohesive bed. *Journal of Fluid Mechanics*, *419*, 203–238. https://doi.org/10.1017/S0022112000001403
Pasternack, G. B., Ellis, C. R., Leier, K. A., Vallé, B. L., & Marr, J. D. (2006). Convergent hydraulics at horseshoe steps in bedrock rivers. *Geomorphology*, *82*(1–2), 126–145. https://doi.org/10.1016/j.geomorph.2005.08.022
Recking, A., Leduc, P., & Liébault, F. (2009). *A Comparison between antidune and step-pool geometries*. IAHR.
Recking, A., Leduc, P., Liébault, F., & Church, M. (2012). A field investigation of the influence of sediment supply on step-pool morphology and stability. *Geomorphology*, *139–140*, 53–66. https://doi.org/10.1016/j.geomorph.2011.09.024
Saletti, M., & Hassan, M. A. (2020). Width variations control the development of grain structuring in steep step-pool dominated streams: Insight from flume experiments. *Earth Surface Processes and Landforms*, *45*(6), 1430–1440. https://doi.org/10.1002/esp.4815
Scheingross, J. S., & Lamb, M. P. (2016). Sediment transport through self-adjusting, bedrock-walled waterfall plunge pools. *Journal of Geophysical Research: Earth Surface*, *121*, 939–963. https://doi.org/10.1002/2015jf003620
Scheingross, J. S., & Lamb, M. P. (2017). A mechanistic model of waterfall plunge pool erosion into bedrock. *Journal of Geophysical Research: Earth Surface*, *122*, 2079–2104. https://doi.org/10.1002/2017JF004195
Scheingross, J. S., Lamb, M. P., & Fuller, B. M. (2019). Self-formed bedrock waterfalls. *Nature*, *567*, 229–233. https://doi.org/10.1038/s41586-019-0991-z
Scheingross, J. S., Lo, D. Y., & Lamb, M. P. (2017). Self-formed waterfall plunge pools in homogeneous rock. *Geophysical Research Letters*, *44*, 200–208. https://doi.org/10.1002/2016GL071730
Slootman, A., & Cartigny, M. J. (2020). Cyclic steps: Review and aggradation-based classification. *Earth-Science Reviews*, *201*(102949), 1–30. https://doi.org/10.1016/j.earscirev.2019.102949
Stein, O. R., Alonso, C. V., & Julien, P. Y. (1993). Mechanics of jet scour downstream of a headcut. *Journal of Hydraulic Research*, *31*(6), 723–738. https://doi.org/10.1080/00221689309498814
Sun, T., & Parker, G. (2005). Transportational cyclic steps created by flow over an erodible bed. Part 2. Theory and numerical simulation. *Journal of Hydraulic Research*, *43*(5), 502–514. https://doi.org/10.1080/00221680509500148
Taki, K., & Parker, G. (2005). Transportational cyclic steps created by flow over an erodible bed. Part 1. Experiments. *Journal of Hydraulic Research*, *43*(5), 488–501. https://doi.org/10.1080/00221680509500147
Teisson, C., Ockenden, M., Le Hir, P., Kranenburg, C., & Hamm, L. (1993). Cohesive sediment transport processes. *Coastal Engineering*, *21*, 129–162. https://doi.org/10.1016/0378-3839(93)90048-D
Umita, T., Kusuda, T., Futawatari, T., & Awaya, Y. (1988). *Study on Erosional Processes of Soft Mud* (Vol. 393, pp. 33–42). Japan Society of Civil Engineering. (in Japanese). https://doi.org/10.2208/jscej.1988.393_33
Wang, L. L., Yao, W. Y., Tang, J. L., Wang, W. L., & Hou, X. X. (2018). Identifying the driving factors of sediment delivery ratio on individual flood events in a long-term monitoring headwater basin. *Journal of Mountain Science*, *15*(8), 1825–1835. https://doi.org/10.1007/s11629-017-4739-7
Wang, X. H., Wang, Y. Q., & Kuznetsov, M. S. (2000). Study on physical properties of several main soils in loess plateau. *Journal of Soil and Water Conservation*, *04*, 99–103. https://doi.org/10.1029/2011WR011436
Waters, K. A., & Curran, J. C. (2012). Investigating step-pool sequence stability. *Water Resources Research*, *48*(W07505), 1–20. https://doi.org/10.1029/2011WR011436
Whittaker, J. G., & Jaeggi, M. N. R. (1982). Origin of step pool system in mountain streams. *Journal of the Hydraulics Division ASCE*, *108*, 758–773. https://doi.org/10.1061/jyceaj.0005873
Wilcox, A. C., Wohl, E. E., Comiti, F., & Mao, L. (2011). Hydraulics, morphology, and energy dissipation in an alpine step-pool channel. *Water Resources Research*, *47*, W07514. https://doi.org/10.1029/2010wr010192
Winterwerp, J. C., Bakker, W. T., Mastbergen, D. R., & van Rossum, H. (1992). Hyperconcentrated sand-water mixture flows over erodible bed. *Journal of Hydraulic Engineering*, *118*(11), 1508–1525. https://doi.org/10.1061/(asce)0733-9429(1992)118:11(1508)
Wohl, E. E., & Grodek, T. (1994). Channel bed-steps along Nahal Yael, Negev desert, Israel. *Geomorphology*, *9*(2), 117–126. https://doi.org/10.1016/0169-555X(94)90070-1
Wohl, E. E., Madsen, S., & MacDonald, L. (1997). Characteristics of log and clast bed-steps in step pool streams of northwestern Montana, USA. *Geomorphology*, *20*, 1–10. https://doi.org/10.1016/S0169-555X(97)00021-4
Wyrick, J. R., & Pasternack, G. B. (2008). Modeling energy dissipation and hydraulic jump regime responses to channel nonuniformity at river steps. *Journal of Geophysical Research: Earth Surface*, *113*, F03003. https://doi.org/10.1029/2007JF000873
Yokokawa, M., Okuno, K., Nakamura, A., Muto, T., Miyata, Y., Naruse, H., & Parker, G. (2009). Aggradational cyclic steps: sedimentary structures found in flume experiments, 33rd International Association for Hydro-Environment Engineering and Research Congress, 5547-5554.
Zeng, Q. C., Li, X., Dong, Y. H., Li, Y., Cheng, M., & An, S. (2015). Ecological stoichiometry characteristics and physical-chemical properties of soils at different latitudes on the Loess Plateau. *Journal of Natural Resources*, *30*(5), 870–879. (In Chinese).
Zimmermann, A., & Church, M. (2001). Channel morphology, gradient profiles and bed stresses during flood in a step-pool channel. *Geomorphology*, *40*(3–4), 311–327. https://doi.org/10.1016/S0169-555X(01)00057-5
Zimmermann, A., Church, M., & Hassan, M. A. (2010). Step-pool stability: Testing the jammed state hypothesis. *Journal of Geophysical Research*, *115*, F02008. https://doi.org/10.1029/2009JF001365

Reference From the Supporting Information

Wu, F. C., Shen, H. W., Chou, Y. J. (1999). Variation of roughness coefficients for unsubmerged and submerged vegetation. *Journal of Hydraulic Engineering*, *125*(9), 934–942. https://doi.org/10.1061/(ASCE)0733-9429(1999)125:9(934)